High repetition rate, multi-MeV proton source from cryogenic hydrogen jets

M. Gauthier, C. B. Curry, S. Göde, F.-E. Brack, J. B. Kim, M. J. MacDonald, J. Metzkes, L. Obst, M. Rehwald, C. Rödel, H.-P. Schlenvoigt, W. Schumaker, U. Schramm, K. Zeil, and S. H. Glenzer

Citation: Appl. Phys. Lett. **111**, 114102 (2017); doi: 10.1063/1.4990487

View online: https://doi.org/10.1063/1.4990487

View Table of Contents: http://aip.scitation.org/toc/apl/111/11

Published by the American Institute of Physics

High repetition rate, multi-MeV proton source from cryogenic hydrogen jets

M. Gauthier,[1,a)] C. B. Curry,[1,2] S. Göde,[1,3] F.-E. Brack,[4,5] J. B. Kim,[1] M. J. MacDonald,[6] J. Metzkes,[4] L. Obst,[4,5] M. Rehwald,[4,5] C. Rödel,[1,7] H.-P. Schlenvoigt,[4] W. Schumaker,[1] U. Schramm,[4,5] K. Zeil,[4] and S. H. Glenzer[1]

[1]*High Energy Density Science Division, SLAC National Accelerator Laboratory, Menlo Park, California 94025, USA*
[2]*University of Alberta, Edmonton, Alberta T6G 1H9, Canada*
[3]*European XFEL GmbH, 22869 Schenefeld, Germany*
[4]*Helmholtz-Zentrum Dresden-Rossendorf, Institute of Radiation Physics, 01328 Dresden, Germany*
[5]*Technische Universität Dresden, 01062 Dresden, Germany*
[6]*University of California Berkeley, Berkeley, California 94720, USA*
[7]*Friedrich-Schiller-University Jena, 07743 Jena, Germany*

(Received 15 June 2017; accepted 2 September 2017; published online 14 September 2017)

We report on a high repetition rate proton source produced by high-intensity laser irradiation of a continuously flowing, cryogenic hydrogen jet. The proton energy spectra are recorded at 1 Hz for Draco laser powers of 6, 20, 40, and 100 TW. The source delivers $\sim 10^{13}$ protons/MeV/sr/min. We find that the average proton number over one minute, at energies sufficiently far from the cut-off energy, is robust to laser-target overlap and nearly constant. This work is therefore a first step towards pulsed laser-driven proton sources for time-resolved radiation damage studies and applications which require quasi-continuous doses at MeV energies. *Published by AIP Publishing.* [http://dx.doi.org/10.1063/1.4990487]

Laser-driven ion acceleration has attracted great interest due to the potential applications in the fast ignition approach to inertial confinement fusion,[1,2] proton radiographic imaging of laser-produced plasmas,[3,4] and stopping power measurements.[5,6] Various other applications in medicine[7–11] and industry[12] have also been explored. In the last two decades, several acceleration mechanisms have been proposed and partially demonstrated.[13] The most robust and studied acceleration mechanism is Target Normal Sheath Acceleration (TNSA). When a high power laser is focused to relativistic intensities on a solid-density foil, relativistic electrons are generated at the front surface and propagate through the target. For micron-thick foils, these electrons escape from the rear surface generating a quasi-static electric field, on the order of TV/m, which accelerates protons and ions from the contaminant layer to MeV energies normal to the target surface.[14,15]

Cryogenic hydrogen jets offer an alternative to conventional metallic foils, generating a pure proton beam without producing debris. The latter becomes increasingly important for high-repetition rate pulsed proton sources. Additionally, the low density and tunable target thickness makes the cryogenic hydrogen jet highly suitable for studying alternative proton acceleration regimes[16,17] predicted to generate higher energy proton beams. Recently, several studies have been conducted on laser-driven proton acceleration from cryogenic hydrogen targets with different laser conditions.[18–21]

In this work, we report on the first experimental demonstration of a 1 Hz pulsed proton source generated from cryogenic hydrogen jets irradiated by the Draco laser at Helmholtz-Zentrum Dresden-Rossendorf (HZDR). The absolute proton energy spectrum recorded at 1 Hz exhibits a semi-Maxwellian energy distribution characteristic of TNSA. The stability of the proton source was investigated by measuring the statistical fluctuations of the proton flux integrated over 1 min at a given energy. Measurements were also collected at several reduced laser powers to study the maximum proton energy scaling for these targets. Furthermore, the advantages of cryogenic jets in high repetition rate experiments are discussed.

The experiment was performed with the Draco short pulse Ti:Sapphire laser system (0.5–3 J, 30 fs, 1 Hz) focused using an f/2.5 off-axis parabola (OAP) to a 3 μm (FWHM) focal spot diameter onto the cryogenic hydrogen jet. This experiment reaches laser intensities of $0.3–5 \times 10^{20}$ W/cm^2 corresponding to a normalized vector potential, $a_0 \simeq 5–21$. The laser contrast was measured with a third-order autocorrelator to be 10^{-7} at -7 ps. A schematic of the experimental set-up is shown in Fig. 1.

The hydrogen jet was generated by a copper assembly cooled by a liquid-helium continuous-flow cryostat. Hydrogen gas is liquefied in the source assembly, cooled to a temperature of 18 K, and then injected through a $\oslash 10$ μm Pt/Ir aperture. In vacuum, the liquid hydrogen continues to cool by evaporative cooling and solidifies before onset of the Plateau-Rayleigh instability.[22] Therefore, the laser interaction region can be up to several centimeters from the source assembly which prevents damage to the aperture from electron heating. At an injection pressure of 2 bar, a jet speed of approximately 70 m/s is expected. We can estimate compatibility of such a target with laser repetition rates up to 1 kHz which greatly exceeds other continuous targets. This estimate assumes a volume element initially in the interaction region has traveled 7 cm away before the arrival of the next laser pulse. It is worth noting that the high repetition rate capabilities of cryogenic hydrogen jets make them ideal targets for experiments combining laser and x-ray free-electron laser (FEL) sources.[23]

[a)]Electronic mail: maxence.gauthier@stanford.edu

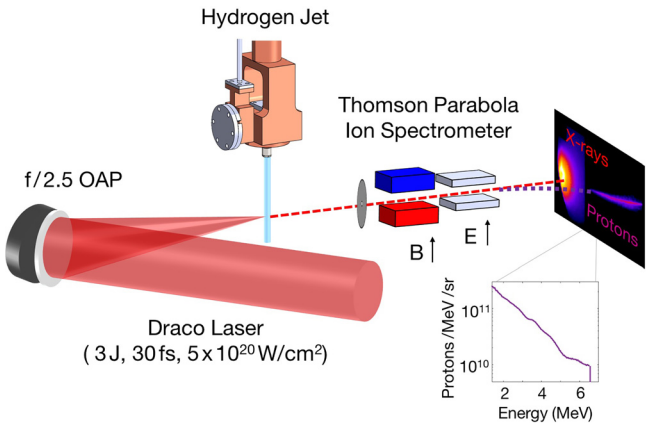

FIG. 1. Schematic of the experimental set-up for 1 Hz proton acceleration from a hydrogen jet. Fast detection Thomson Parabola (TP) ion spectrometers were positioned in the laser forward direction and ±45°. Experimental data of a pure proton spectrum up to 6.5 MeV on the 0° TP is shown. The ±45° TPs and imaging systems are not shown for clarity.

In this study, two f/2 imaging systems operated at 400 nm and 800 nm were used to align the target position relative to the laser focus with micron precision. The spatial jitter of the jet is dominated by angular motion about the aperture output. Consequently, the spatial jitter of the jet in the laser plane increases linearly with distance away from the source aperture. During this experiment, the interaction region was 15 mm below the nozzle where the spatial jitter of the jet position was measured to be approximately ±7 μm.

The proton energy spectrum and flux from the interaction were measured using three energy-calibrated Thomson Parabola (TP) ion spectrometers positioned at 0° and ±45° relative to the laser propagation direction. The 0° TP consisted of a 500 μm pinhole located 0.5 m from the source with a 0.6 T magnetic field to spatially separate the protons by energy. A 40 mm diameter micro-channel plate (MCP) coupled to a phosphor screen and imaged onto a CCD camera allowed fast detection of the proton beam at rates exceeding the laser repetition rate of 1 Hz. The size of the MCP limited the minimum detectable proton energy to ~1.4 MeV.

The signal-to-proton number calibration of the 0° TP was obtained using Radiochromic film (RCF) stacks, consisting of one layer of HD-810 and several of EBT-2,[24] shielded by a 13 μm thick aluminum foil. Each stack was inserted on a single-shot basis in the laser-forward direction (0°) at 55 mm from the proton source covering approximately a ±20° angle. A 3 mm diameter central clearance hole in the RCF allowed simultaneous proton detection by the TP. The calibration compared the RCF dose in each layer to the TP energy spectrum.[25] This method assumes that the MCP efficiency as a function of proton energy is constant.[26] The uncertainty in the calibration is dominated by the spatial non-uniformity of the proton beam[21] giving a systematic uncertainty of ±20% on the absolute proton number.

The proton beams have a semi-Maxwellian energy distribution with a well defined energy cut-off (E_{CO}) typical of TNSA[14] as shown in Fig. 1. Here, the hot electron temperature inferred from the slope of the spectra is ~1 MeV for a measured maximum cut-off energy of 6.5 MeV. Measurements of the proton energy spectra at ±45° indicate TNSA-like emission from cylindrical targets.[21,27] The proton spectra in the laser forward direction, measured at the highest laser intensity (5×10^{20} W/cm^2), for a 1 min series of shots are presented in Fig. 2(a). The stability of the pulsed proton source has been investigated for single-shot and continuous operation.

The proton flux at 3 MeV varies by ~50% from shot-to-shot and the average cut-off energy is 4.0 ± 1.2 MeV following a normal distribution (see supplementary figures). The spread in proton flux and cut-off energy can be explained by: variation in laser energy (<1% RMS); sampling a spatially nonuniform and fluctuating proton beam;[21] or laser-target overlap. In this experiment, the spatial jitter of the jet (7 μm) is comparable to the target radius (5 μm), and expected to be the dominant source of energy fluctuations. In addition, the laser energy coupling is further reduced by any offset from the nominal position due to the projection of the laser on the cylindrical target. To improve the stability of the source, the lateral extent of the target could be increased to several times the spatial jitter of the target; however, such cylindrical hydrogen jets would become too thick for optimal TNSA conditions. Moreover, as the jet flow rate is proportional to the square of the radius, the load on the vacuum system would also increase by a considerable amount. An alternative would be to use a hydrogen ribbon[20] or planar sheet[28] more recently demonstrated on a single-shot basis.

In order to quantify the stability of the pulsed proton source at 1 Hz, the cumulative proton flux for three energies is shown in Figs. 2(b)–2(d). Each data series follows a linear trend, shown in red, with the 95% confidence bounds represented by blue shaded regions. During continuous operation, a small confidence interval indicates that the cumulative proton flux at a particular energy is more predictable and converges towards an ideal pulsed source. After 1 min (60 shots), the uncertainty in the total proton flux at 3, 4, and

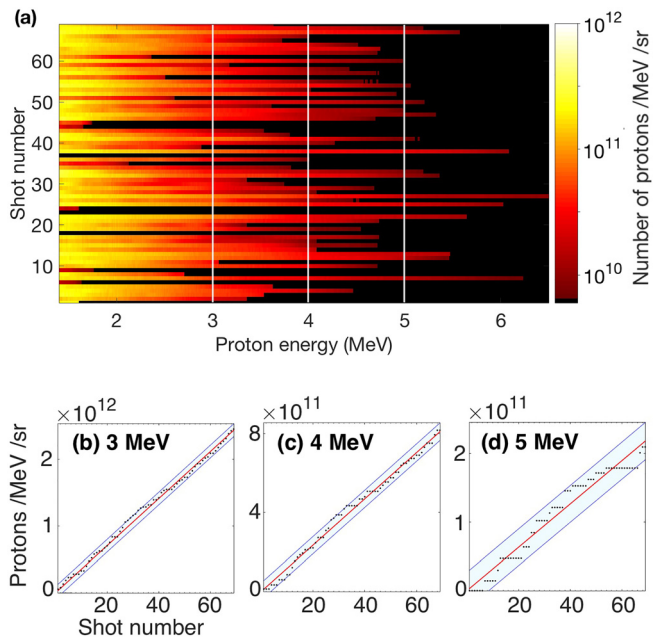

FIG. 2. (a) Proton energy spectrum in the laser forward direction for 68 shots at a laser power of 100 TW recorded at 1 Hz. Cumulative sum of protons at (b) 3 MeV, (c) 4 MeV, and (d) 5 MeV for the same shots. The solid-red line is a linear fit and the 95% confident limits are indicated by the shaded region.

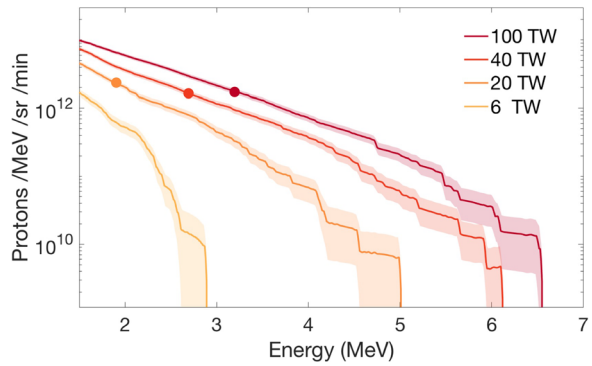

FIG. 3. Integrated proton flux for 6, 20, 40, 100 TW collected at 1 Hz over 1 min. The standard error of the mean is represented by the shaded area. The $0.8\,E_{CO}$ is indicated by filled circles at 1.9 MeV, 2.7 MeV, and 3.2 MeV.

5 MeV becomes ±4.4%, ±6.2%, and ±14%, respectively. Although the proton flux shows important shot-to-shot fluctuations, the accumulation rate stabilizes at energies significantly below the average cut-off energy (<3 MeV) and operation times exceeding 1 min.

The scalability of the maximum proton energy and flux was also studied by measuring the integrated proton energy spectra during 1 Hz operation for laser powers of 6, 20, 40, and 100 TW, by varying the laser energy. A representative sample over 1 min is shown in Fig. 3. Since the hydrogen jet is operable for long periods of time, the sample sets were taken consecutively in order to eliminate other sources of fluctuations. The standard error of the mean (SEM) is represented by the shaded area. For all laser powers, we similarly observe that for energies sufficiently below the average cut-off energy ($0.8\,E_{CO}$), the number of protons at a given energy becomes predictable. For example, the SEM is < 10% for $0.8\,E_{CO}$'s equal to 1.9 MeV, 2.7 MeV, and 3.2 MeV for laser powers of 20 TW, 40 TW, and 100 TW, respectively.

In Fig. 4(a) the maximum cut-off energy from the hydrogen jet for each laser power is plotted. At laser powers <40 TW, we find that our results agree well with, if not exceed, values from micron-thick planar solid-density foils in previous experiments using the Draco laser and other similar laser

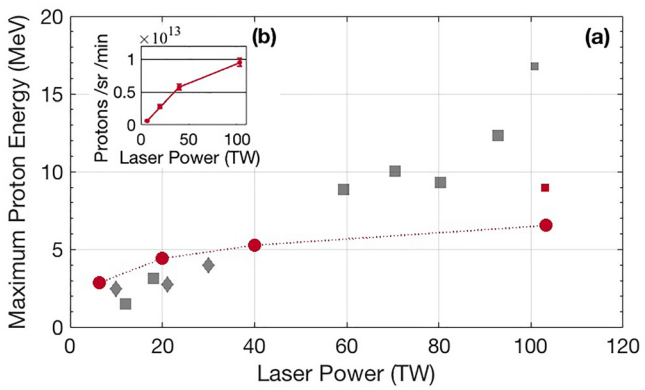

FIG. 4. (a) The maximum proton cut-off energies from this experiment are shown in red. Red circles correspond to shots on the cylindrical hydrogen jet while the small red square is from a 2 μm Ti foil. The small and large gray squares correspond to 2 μm and 5 μm Ti foil shots from previous experiments with the Draco laser.[29] Black diamonds are maximum proton energies from micron-thick foils with comparable ~1 J, 25–40 fs laser systems.[29,30] (b) The number of protons/sr/min are shown as a function of laser power.

systems.[29,30] One explanation for enhanced proton acceleration at low energies is the mass-limited nature of the cylindrical jet.[31,32] In this case, the hot electrons recirculate more efficiently thereby enhancing the magnitude of the electrostatic sheath field.[31] We note that single-shot experiments with nm-thick foils have demonstrated significantly higher proton energies at low laser powers through alternative acceleration mechanisms.[16,30,33,34]

At higher laser powers, however, our spectra are lower than other results from solid-density foils. The cryogenic hydrogen jet, with a density of only 30 n_c and its cylindrical geometry, is expected to be more sensitive to the laser pulse contrast compared with standard foils of comparable thickness. At the arrival time of the main 100 TW laser pulse, the scale-length of the pre-plasma was estimated to be 1–2 μm at the front and rear sides of the cylindrical jet using interferometry. A more detailed discussion of the target expansion during this experiment can be found in Göde *et al.* The lengthening of the density gradient on the target surface, where the TNSA occurs, reduces the electrostatic sheath field, thus decreasing the maximum proton energy.[35] This effect is further confirmed by comparing the maximum proton cut-off energy from a 2 μm thick Ti foil measured during this experiment (9 MeV, small red square) to a previous measurement where the laser contrast was optimized for proton acceleration (17 MeV, small gray square, ps-contrast $< 5 \times 10^{-9}$).[29] As the pre-pulse scales with the laser energy, a smaller expansion is expected at lower laser powers explaining the observed trend.

Similarly, the integrated proton flux within the detection-limit of the TP is plotted with respect to the laser power in Fig. 4(b). The calculated proton number is proportional to the total proton flux, and therefore representative of the conversion efficiency. We find that the proton flux above 1.5 MeV increases linearly with laser power up to 40 TW, in agreement with previous experimental trends.[36,37] At higher powers, the total number of protons increases more gradually, suggesting that the target has suffered significant pre-expansion which degrades TNSA.

Cryogenic hydrogen jets are ideal targets for proton acceleration experiments at high repetition rates facilities as they address two main challenges: target replacement and debris generation. More specifically, the stable proton flux away from the cut-off energy is already suitable for time-resolved radiation damage studies.[38] In addition, the time evolution of microphysical processes occurring in high-intensity laser-plasma interactions can now be investigated at high repetition rate facilities. For example, 100 TW-class laser systems are combined with X-ray free electron lasers (XFELs) such as at the Matter in Extreme Conditions (MECs) end station at SLAC Linac Coherent Light Source (LCLS)[23] or at the future High-Energy-Density (HED) Instrument at European XFEL. To date, several groups have demonstrated continuous tape targets consisting of CH polymers or metals[37,39,40] as well as liquid crystal targets.[41] In comparison to these targets, the hydrogen jet produces a pure proton beam and offers additional flexibility in target thickness and geometry.

Interactions with the hydrogen jet are also debris-free and therefore eliminate the need for debris shielding between

the target and the large optical components in newly available high repetition rate petawatt-class laser systems. Not only must these debris shields exhibit exceptional surface flatness to minimize wavefront error and maintain the laser beam focusability; they must also be sufficiently thin such that B-integral effects are negligible. Debris-free targets, such as cryogenic jets, will therefore decrease the operational costs to routinely replace debris shielding, critical for optimal laser performance.

We demonstrate a stable, 1 Hz proton source delivering $\sim 10^{13}$ protons/MeV/sr/min and a maximum proton energy of 6.5 MeV using a 100 TW laser. Subsequent studies will investigate the required laser contrast, and therefore preplasma scale length, to reach optimal TNSA conditions and higher proton energies with this target. Additionally, planar hydrogen jets will be fielded to improve laser-jet overlap and potentially increase the shot-to-shot reproducibility of the proton energy spectra. This capability is ready for applications in pump-probe experiments[42] and the study of advanced proton acceleration mechanisms[19] at high repetition rates.

See supplementary material for an alternate presentation of the shot-to-shot proton cut-off energy and flux for the data set in Fig. 2(a).

This work was supported by the U.S. Department of Energy Office of Science, Fusion Energy Sciences under FWP 100182. It was also partially supported by EC H2020 LASERLAB-EUROPE/LEPP (Contract No. 654148). C.R. acknowledges support from the Volkswagen Foundation. M.G. and C.C. would like to thank E. E. McBride for fruitful discussions and valuable suggestions.

[1]M. Roth, T. E. Cowan, M. H. Key, S. P. Hatchett, C. Brown, W. Fountain, J. Johnson, D. M. Pennington, R. A. Snavely, S. C. Wilks *et al.*, Phys. Rev. Lett. **86**, 436 (2001).
[2]J. C. Fernández, J. J. Honrubia, B. J. Albright, K. A. Flippo, D. C. Gautier, B. M. Hegelich, M. J. Schmitt, M. Temporal, and L. Yin, Nucl. Fusion **49**, 065004 (2009).
[3]M. Borghesi, D. H. Campbell, A. Schiavi, M. G. Haines, O. Willi, A. J. MacKinnon, P. Patel, L. A. Gizzi, M. Galimberti, R. J. Clarke *et al.*, Phys. Plasmas **9**, 2214 (2002).
[4]L. Romagnani, J. Fuchs, M. Borghesi, P. Antici, P. Audebert, F. Ceccherini, T. Cowan, T. Grismayer, S. Kar, A. Macchi *et al.*, Phys. Rev. Lett. **95**, 195001 (2005).
[5]M. Gauthier, S. N. Chen, A. Levy, P. Audebert, C. Blancard, T. Ceccotti, M. Cerchez, D. Doria, V. Floquet, E. Lamour *et al.*, Phys. Rev. Lett. **110**, 135003 (2013).
[6]A. B. Zylstra, J. A. Frenje, P. E. Grabowski, C. K. Li, G. W. Collins, P. Fitzsimmons, S. Glenzer, F. Graziani, S. B. Hansen, S. X. Hu *et al.*, Phys. Rev. Lett. **114**, 215002 (2015).
[7]S. V. Bulanov, T. Z. Esirkepov, V. S. Khoroshkov, A. V. Kuznetsov, and F. Pegoraro, Phys. Lett. A **299**, 240 (2002).
[8]V. Malka, S. Fritzler, E. Lefebvre, E. d'Humires, R. Ferrand, G. Grillon, C. Albaret, S. Meyroneinc, J.-P. Chambaret, A. Antonetti *et al.*, Med. Phys. **31**, 1587 (2004).
[9]T. Tajima, D. Habs, and X. Yan, Rev. Accel. Sci. Technol. **2**, 201 (2009).
[10]S. D. Kraft, C. Richter, K. Zeil, M. Baumann, E. Beyreuther, S. Bock, M. Bussmann, T. E. Cowan, Y. Dammene, W. Enghardt *et al.*, New J. Phys. **12**, 085003 (2010).
[11]K. Zeil, M. Baumann, E. Beyreuther, T. Burris-Mog, T. E. Cowan, W. Enghardt, L. Karsch, S. D. Kraft, L. Laschinsky, J. Metzkes *et al.*, Appl. Phys. B **110**, 437 (2013).
[12]M. Rosiński, J. Badziak, F. Boody, S. Gammino, H. Hora, J. Krása, L. Láska, A. Mezzasalma, P. Parys, K. Rohlena *et al.*, Vacuum **78**, 435 (2005).
[13]A. Macchi, M. Borghesi, and M. Passoni, Rev. Mod. Phys. **85**, 751 (2013).
[14]P. Mora, Phys. Rev. Lett. **90**, 185002 (2003).
[15]R. A. Snavely, M. H. Key, S. P. Hatchett, I. E. Cowan, M. Roth, T. W. Phillips, M. A. Stoyer, E. A. Henry, T. C. Sangster, M. S. Singh *et al.*, Phys. Rev. Lett. **85**, 2945 (2000).
[16]A. Henig, S. Steinke, M. Schnürer, T. Sokollik, R. Hörlein, D. Kiefer, D. Jung, J. Schreiber, B. M. Hegelich, X. Q. Yan *et al.*, Phys. Rev. Lett. **103**, 245003 (2009).
[17]D. Haberberger, S. Tochitsky, F. Fiuza, C. Gong, R. A. Fonseca, L. O. Silva, W. B. Mori, and C. Joshi, Nat. Phys. **8**, 95 (2012).
[18]R. A. Costa-Fraga, A. Kalinin, M. Khnel, D. C. Hochhaus, A. Schottelius, J. Polz, M. C. Kaluza, P. Neumayer, and R. E. Grisenti, Rev. Sci. Instrum. **83**, 025102 (2012).
[19]M. Gauthier, J. B. Kim, C. B. Curry, B. Aurand, E. J. Gamboa, S. Göde, C. Goyon, A. Hazi, S. Kerr, A. Pak *et al.*, Rev. Sci. Instrum. **87**, 11D827 (2016).
[20]D. Margarone, A. Velyhan, J. Dostal, J. Ullschmied, J. P. Perin, D. Chatain, S. Garcia, P. Bonnay, T. Pisarczyk, R. Dudzak *et al.*, Phys. Rev. X **6**, 041030 (2016).
[21]S. Göde, C. Rödel, K. Zeil, R. Mishra, M. Gauthier, F.-E. Brack, T. Kluge, M. J. MacDonald, J. Metzkes, L. Obst *et al.*, Phys. Rev. Lett. **118**, 194801 (2017).
[22]J. B. Kim, S. Göde, and S. H. Glenzer, Rev. Sci. Instrum. **87**, 11E328 (2016).
[23]S. H. Glenzer, L. B. Fletcher, E. Galtier, B. Nagler, R. Alonso-Mori, B. Barbrel, S. B. Brown, D. A. Chapman, Z. Chen, C. B. Curry *et al.*, J. Phys. B: At., Mol. Opt. Phys. **49**, 092001 (2016).
[24]Ashland, "GAFchromic Radiology Films" (2017).
[25]A. Mancicć, J. Fuchs, P. Antici, S. A. Gaillard, and P. Audebert, Rev. Sci. Instrum. **79**, 073301 (2008).
[26]T. W. Jeong, P. K. Singh, C. Scullion, H. Ahmed, K. F. Kakolee, P. Hadjisolomou, A. Alejo, S. Kar, M. Borghesi, and S. Ter-Avetisyan, Rev. Sci. Instrum. **87**, 083301 (2016).
[27]M. Roth, A. Blazevic, M. Geissel, T. Schlegel, T. E. Cowan, M. Allen, J.-C. Gauthier, P. Audebert, J. Fuchs, J. Meyer-ter Vehn *et al.*, Phys. Rev. Spec. Top.–Accel. Beams **5**, 061301 (2002).
[28]L. Obst, S. Göde, M. Rehwald, F.-E. Brack, J. Branco, S. Bock, M. Bussmann, T. E. Cowan, C. B. Curry, F. Fiuza, *et al.*, Sci. Rep. **7**, 10248 (2017).
[29]K. Zeil, S. D. Kraft, S. Bock, M. Bussmann, T. E. Cowan, T. Kluge, J. Metzkes, T. Richter, R. Sauerbrey, and U. Schramm, New J. Phys. **12**, 045015 (2010).
[30]A. Macchi, A. Sgattoni, S. Sinigardi, M. Borghesi, and M. Passoni, Plasma Phys. Controlled Fusion **55**, 124020 (2013).
[31]K. Zeil, J. Metzkes, T. Kluge, M. Bussmann, T. E. Cowan, S. D. Kraft, R. Sauerbrey, B. Schmidt, M. Zier, and U. Schramm, Plasma Phys. Controlled Fusion **56**, 084004 (2014).
[32]T. Kluge, W. Enghardt, S. D. Kraft, U. Schramm, K. Zeil, T. E. Cowan, and M. Bussmann, Phys. Plasmas **17**, 123103 (2010).
[33]D. Neely, P. Foster, A. Robinson, F. Lindau, O. Lundh, A. Persson, C.-G. Wahlstrm, and P. McKenna, Appl. Phys. Lett. **89**, 021502 (2006).
[34]B. M. Hegelich, I. Pomerantz, L. Yin, H. C. Wu, D. Jung, B. J. Albright, D. C. Gautier, S. Letzring, S. Palaniyappan, R. Shah *et al.*, New J. Phys. **15**, 085015 (2013).
[35]M. Kaluza, J. Schreiber, M. I. K. Santala, G. D. Tsakiris, K. Eidmann, J. Meyer-ter Vehn, and K. J. Witte, Phys. Rev. Lett. **93**, 045003 (2004).
[36]J. Fuchs, P. Antici, E. D'Humières, E. Lefebvre, M. Borghesi, E. Brambrink, C. A. Cecchetti, M. Kaluza, V. Malka, M. Manclossi *et al.*, Nat. Phys. **2**, 48 (2006).
[37]J. Schreiber, P. R. Bolton, and K. Parodi, Rev. Sci. Instrum. **87**, 071101 (2016).
[38]B. Dromey, M. Coughlan, L. Senje, M. Taylor, S. Kuschel, B. Villagomez-Bernabe, R. Stefanuik, G. Nersisyan, L. Stella, J. Kohanoff *et al.*, Nat. Commun. **7**, 10642 (2016).
[39]M. Noaman-ul Haq, H. Ahmed, T. Sokollik, L. Yu, Z. Liu, X. Yuan, F. Yuan, M. Mirzaie, X. Ge, L. Chen *et al.*, Phys. Rev. Spec. Top.–Accel. Beams **20**, 041301 (2017).
[40]A. S. Pirozhkov, M. Mori, A. Yogo, H. Kiriyama, K. Ogura, A. Sagisaka, J.-L. Ma, S. Orimo, M. Nishiuchi, H. Sugiyama *et al.*, Proc. SPIE **7354**, 735414 (2009).
[41]P. L. Poole, A. Krygier, G. E. Cochran, P. S. Foster, G. G. Scott, L. A. Wilson, J. Bailey, N. Bourgeois, C. Hernandez-Gomez, D. Neely *et al.*, Sci. Rep. **6**, 32041 (2016).
[42]L. B. Fletcher, U. Zastrau, E. Galtier, E. J. Gamboa, S. Goede, W. Schumaker, A. Ravasio, M. Gauthier, M. J. MacDonald, Z. Chen *et al.*, Rev. Sci. Instrum. **87**, 11E524 (2016).